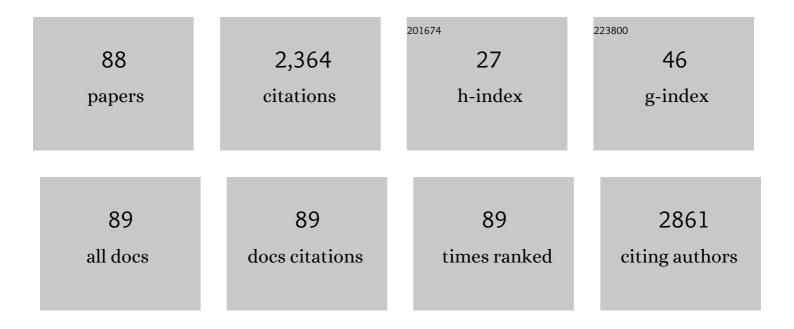
## List of Publications by Year in descending order

Source: https://exaly.com/author-pdf/1307508/publications.pdf Version: 2024-02-01



ΟΠΑΝΤΗ

#	Article	IF	CITATIONS
1	Review of Monte Carlo modeling of light transport in tissues. Journal of Biomedical Optics, 2013, 18, 050902.	2.6	253
2	Review of Fluorescence Suppression Techniques in Raman Spectroscopy. Applied Spectroscopy Reviews, 2015, 50, 387-406.	6.7	201
3	Comparison of principal component analysis and biochemical component analysis in Raman spectroscopy for the discrimination of apoptosis and necrosis in K562 leukemia cells. Optics Express, 2012, 20, 22158.	3.4	127
4	Effect of fiber optic probe geometry on depth-resolved fluorescence measurements from epithelial tissues: a Monte Carlo simulation. Journal of Biomedical Optics, 2003, 8, 237.	2.6	84
5	Experimental validation of Monte Carlo modeling of fluorescence in tissues in the UV-visible spectrum. Journal of Biomedical Optics, 2003, 8, 223.	2.6	83
6	Sequential estimation of optical properties of a two-layered epithelial tissue model from depth-resolved ultraviolet-visible diffuse reflectance spectra. Applied Optics, 2006, 45, 4776.	2.1	70
7	Surface Enhanced Raman Spectroscopy Based Biosensor with a Microneedle Array for Minimally Invasive <i>In Vivo</i> Glucose Measurements. ACS Sensors, 2020, 5, 1777-1785.	7.8	69
8	Magnetic field enriched surface enhanced resonance Raman spectroscopy for early malaria diagnosis. Journal of Biomedical Optics, 2012, 17, 017005.	2.6	68
9	Relationship between depth of a target in a turbid medium and fluorescence measured by a variable-aperture method. Optics Letters, 2002, 27, 104.	3.3	66
10	Recovery of Raman spectra with low signal-to-noise ratio using Wiener estimation. Optics Express, 2014, 22, 12102.	3.4	66
11	Investigation of fiber-optic probe designs for optical spectroscopic diagnosis of epithelial pre-cancers. Lasers in Surgery and Medicine, 2004, 34, 25-38.	2.1	65
12	Scaling method for fast Monte Carlo simulation of diffuse reflectance spectra from multilayered turbid media. Journal of the Optical Society of America A: Optics and Image Science, and Vision, 2007, 24, 1011.	1.5	63
13	Compact point-detection fluorescence spectroscopy system for quantifying intrinsic fluorescence redox ratio in brain cancer diagnostics. Journal of Biomedical Optics, 2011, 16, 037004.	2.6	51
14	Experimental proof of the feasibility of using an angled fiber-optic probe for depth-sensitive fluorescence spectroscopy of turbid media. Optics Letters, 2004, 29, 2034.	3.3	50
15	Roles of linear and circular polarization properties and effect of wavelength choice on differentiation between <i>ex vivo</i> normal and cancerous gastric samples. Journal of Biomedical Optics, 2014, 19, 046020.	2.6	50
16	Towards ultrasensitive malaria diagnosis using surface enhanced Raman spectroscopy. Scientific Reports, 2016, 6, 20177.	3.3	48
17	A narrow-bandgap benzobisthiadiazole derivative with high near-infrared photothermal conversion efficiency and robust photostability for cancer therapy. Chemical Communications, 2015, 51, 4223-4226.	4.1	45
18	Modified Wiener estimation of diffuse reflectance spectra from RGB values by the synthesis of new colors for tissue measurements. Journal of Biomedical Optics, 2012, 17, 030501.	2.6	44

#	Article	IF	CITATIONS
19	Role of optical spectroscopy using endogenous contrasts in clinical cancer diagnosis. World Journal of Clinical Oncology, 2011, 2, 50.	2.3	42
20	Graphene quantum dot based chargeâ€reversal nanomaterial for nucleusâ€targeted drug delivery and efficiency controllable photodynamic therapy. Journal of Biophotonics, 2019, 12, e201800367.	2.3	42
21	Dual functions of gold nanorods as photothermal agent and autofluorescence enhancer to track cell death during plasmonic photothermal therapy. Cancer Letters, 2015, 357, 152-159.	7.2	40
22	Sustained and Cost Effective Silver Substrate for Surface Enhanced Raman Spectroscopy Based Biosensing. Scientific Reports, 2017, 7, 6917.	3.3	37
23	Optimization in interstitial plasmonic photothermal therapy for treatment planning. Medical Physics, 2013, 40, 103301.	3.0	36
24	Towards <i>in vivo</i> intradermal surface enhanced Raman scattering (SERS) measurements: silver coated microneedle based SERS probe. Journal of Biophotonics, 2014, 7, 683-689.	2.3	36
25	Stepwise method based on Wiener estimation for spectral reconstruction in spectroscopic Raman imaging. Optics Express, 2017, 25, 1005.	3.4	34
26	Optimization of Fe3O4@Ag nanoshells in magnetic field-enriched surface-enhanced resonance Raman scattering for malaria diagnosis. Analyst, The, 2013, 138, 6494-6500.	3.5	32
27	Development of a synchronous fluorescence imaging system and data analysis methods. Optics Express, 2007, 15, 12583.	3.4	29
28	Non-invasive controlled release from gold nanoparticle integrated photo-responsive liposomes through pulse laser induced microbubble cavitation. Colloids and Surfaces B: Biointerfaces, 2015, 126, 569-574.	5.0	29
29	Spectral filtering modulation method for estimation of hemoglobin concentration and oxygenation based on a single fluorescence emission spectrum in tissue phantoms. Medical Physics, 2009, 36, 4819-4829.	3.0	26
30	Fast reconstruction of Raman spectra from narrowâ€band measurements based on Wiener estimation. Journal of Raman Spectroscopy, 2013, 44, 875-881.	2.5	25
31	Investigation on the potential of Mueller matrix imaging for digital staining. Journal of Biophotonics, 2016, 9, 364-375.	2.3	24
32	Investigation of Synchronous Fluorescence Method in Multicomponent Analysis in Tissue. IEEE Journal of Selected Topics in Quantum Electronics, 2010, 16, 927-940.	2.9	23
33	Validity of the semi-infinite tumor model in diffuse reflectance spectroscopy for epithelial cancer diagnosis: a Monte Carlo study. Optics Express, 2011, 19, 17799.	3.4	23
34	Hollow agarose microneedle with silver coating for intradermal surface-enhanced Raman measurements: a skin-mimicking phantom study. Journal of Biomedical Optics, 2015, 20, 061102.	2.6	23
35	Fast photoacoustic-guided depth-resolved Raman spectroscopy: a feasibility study. Optics Letters, 2015, 40, 3568.	3.3	23
36	Axicon lens-based cone shell configuration for depth-sensitive fluorescence measurements in turbid media. Optics Letters, 2013, 38, 2647.	3.3	21

#	Article	IF	CITATIONS
37	Raman Spectroscopy Based Techniques in Tissue Engineering—An Overview. Applied Spectroscopy Reviews, 2014, 49, 513-532.	6.7	20
38	Fast hydrothermal co-liquefaction of corn stover and cow manure for biocrude and hydrochar production. Bioresource Technology, 2021, 340, 125630.	9.6	19
39	Hybrid method for fast Monte Carlo simulation of diffuse reflectance from a multilayered tissue model with tumor-like heterogeneities. Journal of Biomedical Optics, 2012, 17, 010501.	2.6	18
40	Optimization of advanced Wiener estimation methods for Raman reconstruction from narrow-band measurements in the presence of fluorescence background. Biomedical Optics Express, 2015, 6, 2633.	2.9	18
41	Fast wide-field Raman spectroscopic imaging based on simultaneous multi-channel image acquisition and Wiener estimation. Optics Letters, 2016, 41, 2783.	3.3	18
42	Comparison of principal component analysis and biochemical component analysis in Raman spectroscopy for the discrimination of apoptosis and necrosis in K562 leukemia cells: errata. Optics Express, 2012, 20, 25041.	3.4	16
43	Numerical investigation of lens based setup for depth sensitive diffuse reflectance measurements in an epithelial cancer model. Optics Express, 2012, 20, 29807.	3.4	16
44	Theranostic Colloidal Nanoparticles of Pyrrolopyrrole Cyanine Derivatives for Simultaneous Near-Infrared Fluorescence Cancer Imaging and Photothermal Therapy. ACS Applied Bio Materials, 2018, 1, 1109-1117.	4.6	15
45	Early Prediction of Skin Viability Using Visible Diffuse Reflectance Spectroscopy and Autofluorescence Spectroscopy. Plastic and Reconstructive Surgery, 2014, 134, 240e-247e.	1.4	14
46	Snapshot depth sensitive Raman spectroscopy in layered tissues. Optics Express, 2016, 24, 28312.	3.4	13
47	Review of Surface Enhanced Raman Spectroscopy for Malaria Diagnosis and a New Approach for the Detection of Single Parasites in the Ring Stage. IEEE Journal of Selected Topics in Quantum Electronics, 2016, 22, 179-187.	2.9	13
48	A Fast Fluorescence Background Suppression Method for Raman Spectroscopy Based on Stepwise Spectral Reconstruction. IEEE Access, 2018, 6, 67709-67717.	4.2	13
49	Laser-Induced Surface Acoustic Wave Sensing-Based Malaria Parasite Detection and Analysis. IEEE Transactions on Instrumentation and Measurement, 2022, 71, 1-9.	4.7	12
50	Early detection and differentiation of venous and arterial occlusion in skin flaps using visible diffuse reflectance spectroscopy and autofluorescence spectroscopy. Biomedical Optics Express, 2016, 7, 570.	2.9	11
51	Synthesis and in vivo magnetic resonance imaging evaluation of biocompatible branched copolymer nanocontrast agents. International Journal of Nanomedicine, 2015, 10, 5895.	6.7	9
52	Spectral diffuse reflectance and autofluorescence imaging can perform early prediction of blood vessel occlusion in skin flaps. Journal of Biophotonics, 2017, 10, 1665-1675.	2.3	9
53	Fast depth-sensitive fluorescence measurements in turbid media using cone shell configuration. Journal of Biomedical Optics, 2013, 18, 110503.	2.6	8
54	Modeling of nonphase mechanisms in ultrasonic modulation of light propagation. Applied Optics, 2008, 47, 3619.	2.1	7

#	Article	IF	CITATIONS
55	Phantom validation of Monte Carlo modeling for noncontact depth sensitive fluorescence measurements in an epithelial tissue model. Journal of Biomedical Optics, 2014, 19, 085006.	2.6	7
56	Hadamard transform-based calibration method for programmable optical filters based on digital micro-mirror device. Optics Express, 2018, 26, 19563.	3.4	7
57	A Method to Create a Universal Calibration Dataset for Raman Reconstruction Based on Wiener Estimation. IEEE Journal of Selected Topics in Quantum Electronics, 2016, 22, 164-170.	2.9	6
58	Denoising Raman spectra by Wiener estimation with a numerical calibration dataset. Biomedical Optics Express, 2020, 11, 200.	2.9	6
59	Multifocal noncontact color imaging for depth-sensitive fluorescence measurements of epithelial cancer. Optics Letters, 2014, 39, 3250.	3.3	5
60	Cell Membrane-Coated Electrospun Fibers Enhance Keratinocyte Growth through Cell-Type Specific Interactions. ACS Applied Bio Materials, 2021, 4, 4079-4083.	4.6	5
61	Depth-sensitive Raman spectroscopy for skin wound evaluation in rodents. Biomedical Optics Express, 2019, 10, 6114.	2.9	5
62	Sequential weighted Wiener estimation for extraction of key tissue parameters in color imaging: a phantom study. Journal of Biomedical Optics, 2014, 19, 127001.	2.6	4
63	Improving Depth Sensitive Fluorescence Spectroscopy With Wavefront Shaping by Spectral and Spatial Filtering. IEEE Access, 2019, 7, 170192-170198.	4.2	4
64	Polarized Raman spectroscopy for enhanced quantification of protein concentrations in an aqueous mixture. Journal of Raman Spectroscopy, 2015, 46, 744-749.	2.5	3
65	Efficiency enhancement of Raman spectroscopy at long working distance by parabolic reflector. Biomedical Optics Express, 2017, 8, 5243.	2.9	3
66	Compressive Optical Spectrometry Based on Sequency-Ordered Hadamard Transform. IEEE Photonics Journal, 2020, 12, 1-8.	2.0	3
67	A Modified Least-Squares Method for Quantitative Analysis in Raman Spectroscopy. IEEE Journal of Selected Topics in Quantum Electronics, 2021, 27, 1-9.	2.9	2
68	Optical coherence tomography-guided confocal Raman microspectroscopy for rapid measurements in tissues. Biomedical Optics Express, 2022, 13, 344.	2.9	2
69	A scaling Monte Carlo method for diffuse reflectance computation from multi-layered media. , 2007, , .		1
70	Validity of the semi-infinite tumor model in tissue optics: A Monte Carlo study. , 2010, , .		1
71	Towards field malaria diagnosis using surface enhanced Raman spectroscopy. , 2016, , .		1
72	Investigation of surface enhanced Raman spectroscopy for hemozoin detection in malaria diagnosis. , 2016, , .		1

#	Article	IF	CITATIONS
73	Towards malaria field diagnosis based on surface-enhanced Raman scattering with on-chip sample preparation and near-analyte nanoparticle synthesis. Sensors and Actuators B: Chemical, 2021, 343, 130162.	7.8	1
74	Malaria diagnosis using magnetic nanoparticles. , 2010, , .		0
75	Fast reconstruction of Raman spectra from narrow-band measurements based on Wiener estimation. , 2012, , .		0
76	A hybrid method for fast Monte Carlo simulation of diffuse reflectance from a multi-layered tissue model with tumor-like heterogeneities. , 2012, , .		0
77	Numerical and experimental investigation of lens based configurations for depth sensitive optical measurements. , 2013, , .		0
78	Comparison of cone and cone shell configuration for depth sensitive fluorescence measurements in turbid media. , 2014, , .		0
79	Investigation of magnetic field enriched surface enhanced resonance Raman scattering performance using Fe <sub>3</sub> O <sub>4</sub> @Ag nanoparticles for malaria diagnosis. Proceedings of SPIE, 2014, , .	0.8	0
80	Cold nanorods as photothermal agents and autofluorescence enhancer to track cell death during plasmonic photothermal therapy. , 2015, , .		0
81	Efficiency enhancement of Raman microspectroscopy at long working distance by parabolic reflector. , 2017, , .		0
82	Monte Carlo based inverse model of diffuse reflectance for determination of UV-VIS optical properties and its application to breast cancer diagnosis. , 2004, , .		0
83	Angled probe design for scattering measurements from a small tissue volume. , 2006, , .		0
84	Cold nanorods as photothermal agents and autofluorescence enhancer to track cell death during plasmonic photothermal therapy. , 2015, , .		0
85	Fast wide-field Raman spectroscopic imaging based on multi-channel narrow-band imaging and Wiener estimation. , 2018, , .		0
86	Surface enhanced Raman spectroscopy for malaria diagnosis and intradermal measurements. , 2018, , .		0
87	Depth sensitive Raman spectroscopy for skin wounds in rodents. , 2019, , .		0
88	Improving depth sensitive fluorescence spectroscopy with wavefront shaping. , 2019, , .		0